Characteristic Modeling of the Wear Particle Formation Process from a Tribological Testing of Polyethylene with Controlled Surface Asperities

Hsu-Wei Fang

Department of Chemical Engineering and Biotechnology, National Taipei University of Technology, Taipei, Taiwan

Received 9 June 2006; accepted 7 July 2006
DOI 10.1002/app.25210
Published online in Wiley InterScience (www.interscience.wiley.com).

ABSTRACT: To study the ultra-high molecular weight polyethylene (UHMWPE) wear particles-induced osteolysis which leads to the failure of artificial joints, microfabricated surfaces with controlled asperities have been applied to generate narrowly distributed UHMWPE wear particles with various sizes and shapes. Our previous study further facilitated single wedge sliding tests to investigate the mechanism of the UHMWPE particle generation. In this study, the attempt was made to characterize the particle generation process into a mathematical model to predict particle volume with a given surface-texture dimensions and mechanical loading conditions. The particle-generation process is decomposed into two steps: (1) penetration of the cutting edge, and (2) lateral sliding of the cutting edge. By combining the indentation experimental data, the viscoelastic responses of UHMWPE was incorporated in the model. The effects of normal load, feature height, and cutting edge angle on the wear particle volume were illustrated from model predictions. Both experimental results and model predictions indicate the same trend of effects of surface-texture geometry and mechanical conditions on the volume of particles. The results of the model predictions are close to the experimental results of the particle generation. However, the particle volume predicted by the model is larger than the experimental results. It is believed that the reprocessing of the generated particles and viscoelastic recovery of UHMWPE in the experiments account for this difference. © 2006 Wiley Periodicals, Inc. J Appl Polym Sci 103: 587–594, 2007

Key words: UHMWPE; wear particles; modeling; surface texture; controlled asperities; viscoelasticity

INTRODUCTION

Tribology has emerged as a critical phenomenon in the biological and medical applications in recent years. Wear and wear particles of ultra-high molecular weight polyethylene (UHMWPE) induced immunological responses have been identified as the major reasons causing the failure of the joint prostheses.[1–3] To study the effects of size and shape of wear particles on the immunological responses, a wear testing procedure by rubbing UHMWPE with controlled asperities on the surfaces has been developed to generate UHMWPE wear particles with controlled sizes and shapes.[4–6] Figure 1 shows the micro-cutting process of the UHMWPE particle generation. The wedge features were fabricated on the silicon surface. By rubbing UHMWPE with silicon surfaces with wedge features, the mass production of the particles can be achieved, and the particle size and shape can be controlled by the dimensions of the surface features and the mechanical conditions of the rubbing process. Microfabricated surface textures with various dimensions have been designed and prepared for UHMWPE particle generation.[4] Figure 2 shows the micrographs of various surface features along with the generated UHMWPE particles under the same contact pressure of 3 MPa and average sliding speed of 57.2 mm/s in water.[5]

The morphology of the worn surface and the wear particles of UHMWPE have been observed after the particle-generation process. Figure 3 shows an example of SEM photos of the UHMWPE worn surface, the single surface feature, and generated particles. Shear deformation of UHMWPE were observed along the sliding direction.[6] The width of the sliding track seen on the worn surface is consistent with the length of the cutting edge. On the basis of this observation, the mechanism of the particles has been proposed which is generated from the following steps:[7] (a) deformation of the material due to the penetration and sliding processes of the surface features; (b) strain hardening occurs under a surface-feature sliding process; (c) UHMWPE molecules align to the direction where the shear stress is applied and the surface layer of material becomes more brittle; (d) detachment of the particle at the tip edge-

Correspondence to: H.-W. Fang (hwfang@ntut.edu.tw).
Contract grant sponsor: National Science Council; contract grant number: NSC 94-2213-E-027-002.

Journal of Applied Polymer Science, Vol. 103, 587–594 (2007)

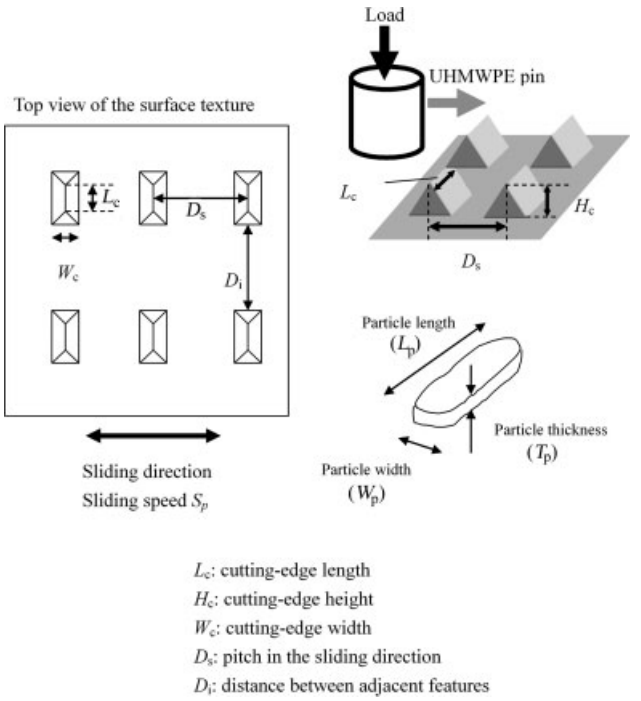

Figure 1 Illustrations of significant variables for the particle-generation process.

material interface, according to the fracture of UHWMPE. Single tip sliding experiments have been designed to investigate the kinematics and the material response of the UHMWPE particle-generation process.[7] From *in situ* observation of the process, the kinematics of the surface feature micro-cutting process has been elucidated.

In this study, we attempt to characterize the particle generation process into a mathematical model to predict particle volume with a given surface-texture dimensions and mechanical loading conditions. The particle-generation process is decomposed into two steps: (1) penetration of the cutting edge, and (2) lateral sliding of the cutting edge. The penetration depth of a wedge-shaped cutting edge is calculated based on the force equilibrium in Newton's principle. During the sliding of the cutting edges, displaced volume of UHMWPE leads to the material resistant force acting on the cutting edges. The resolved component force in the vertical direction lifts up the cutting edge. The penetration depth then decreases as the tip travels further. The balance of forces between the normal load and the lift-up force contributed from the material resistance is then finally reached. We are going to calculate the displaced volume of UHMWPE during the sliding process. The volume is projected to be the volume of generated particles. Finally, a model is developed to determine the shear volume (displaced volume) of UHMWPE with given surface texture geometry and mechanical loading condition.

MODEL

The variables of the model are the dimensions of the surface texture, the mechanical operation parameters, and the particle dimensions as output variables. A schematic representation of the particle-generation process is shown in Figure 1. The important dimensions of the surface texture include the cutting-edge feature length (L_c), the feature width (W_c), the feature height (H_c), the distance between features along the sliding direction (D_s), and the distance between adjacent features (D_i). Two mechanical operation parameters during the linear reciprocating wear process are the load applied on each cutting-edge feature (W), and average sliding speed (S_p). Based on the sheet-like morphology generated from this process, the particle is characterized as the particle length (L_p), the particle width (W_p), and the particle thickness (T_p), and then the particle volume (V_p) is estimated by the product of these three dimensions.

Penetration of the cutting edge

The penetration process of the cutting edge is discussed as a wedge indentation process. A schematic representation is shown in Figure 4. The key parameters shown in the figure include the cutting-edge length (L_c), half angle of the cutting edge (θ), average normal load on each feature (W), and the penetration depth (H_p). Theoretical calculations of the penetration depth of a wedge tip with purely plastic and elastic-plastic assumptions have been carried out earlier.[8,9] As shown in Figure 4, the average normal load acting on each cutting edge is W. The contact length after the indentation process is $2H_p \tan\theta$. The average contact pressure applied to the material can be calculated by:

$$\text{Average contact pressure } p_{\text{pen}} = \frac{W}{2L_c H_p \tan\theta} \quad (1)$$

With the perfect plastic deformation assumption, no deformation will occur until the yield stress is reached, after which plastic flow occurs. The relationship between average contact pressure and the yield stress has the following relationship:[8]

$$p_{\text{pen}} = C_p Y \quad (2)$$

where C_p is a coefficient for different geometry of the indenter. For a wedge-shaped indenter, the C_p is a function of θ and is described as[9]

$$C_p = \lambda[2.57 - 0.023(90 - \theta)] \quad (3)$$

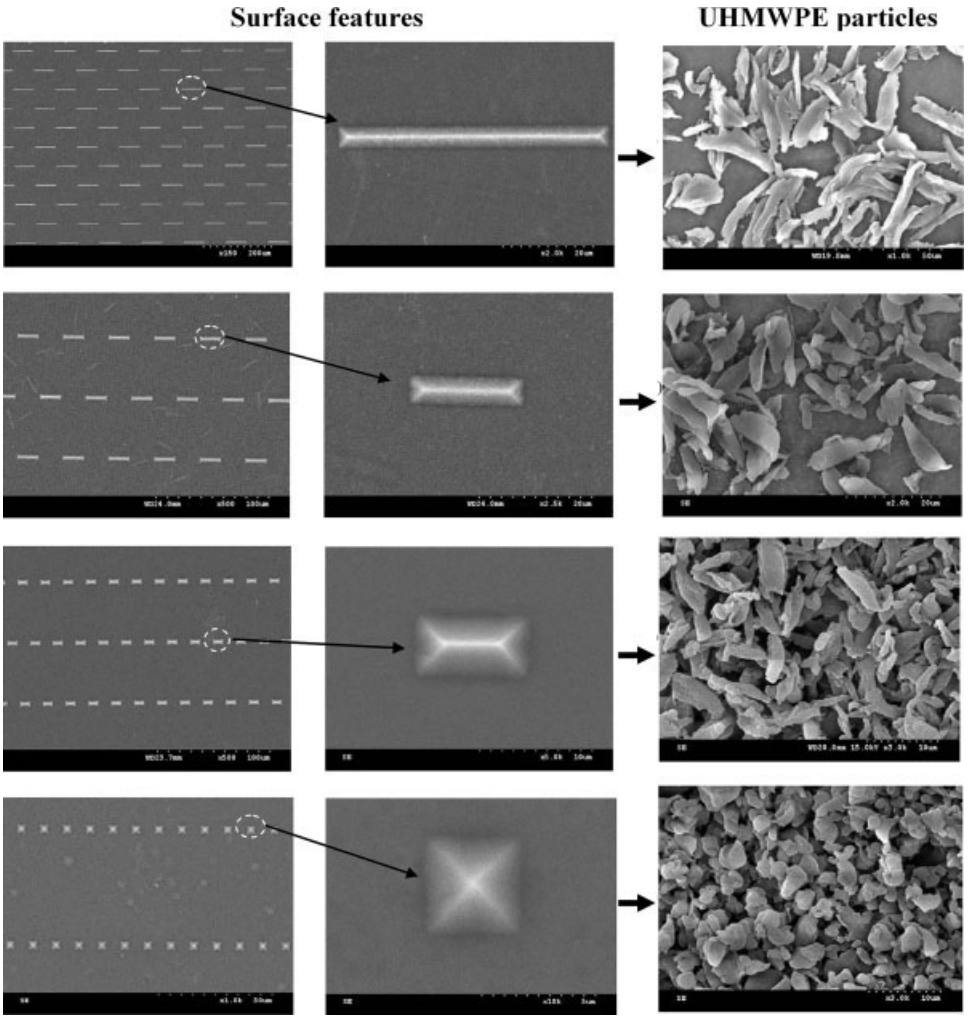

Figure 2 Micrographs of the surface textures and generated UHMWPE particles.

where $\lambda = 2/\sqrt{3}$ by the von Mises yield criterion, and where θ is expressed in degrees. By balancing the pressure in the z direction, we obtain:

$$\frac{W}{2L_c H_p \tan\theta} = C_p Y \tag{4}$$

Thus the penetration depth ($H_{p,p}$) predicted by the purely plastic hypothesis can be expressed as

$$H_{p,p} = \frac{W}{2(C_p Y) L_c \tan\theta} \tag{5}$$

where Y is the yield strength of the material.

With an elastic-plastic assumption of the material property, a certain amount of deformation will be recovered after the applied stress is released. Johnson[9] has derived that H/Y (H: hardness, Y: yield strength) is a function of penetration depth and E/Y (E: elastic

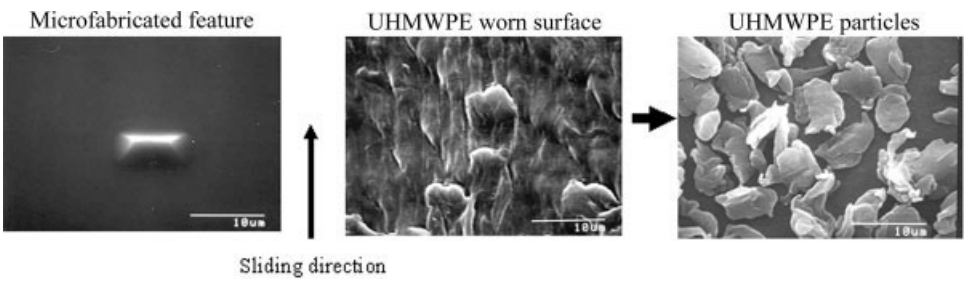

Figure 3 SEM micrographs of surface cutting-edge feature, UHMWPE worn surface, and generated UHMWPE particles.

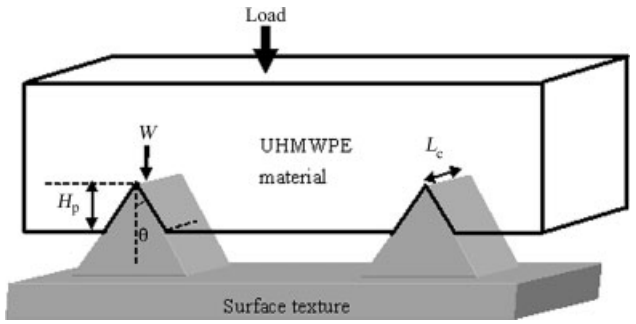

Figure 4 Schematic of the penetration process of the cutting edges.

modulus). By representing hardness by the normal force and the size of deformation site after penetration, the predicted penetration depth with elastic-plastic assumption can be described as:

$$H_{p,\mathrm{ep}} = \frac{W}{2(C_{\mathrm{ep}}Y)L_c \tan\theta} \tag{6}$$

where C_{ep} is a function of material property and penetration edge geometry. For a wedge geometry, C_{ep} is derived by Johnson[9] as following:

$$C_{\mathrm{ep}} = \frac{1}{\sqrt{3}} \times \left[1 + \ln\left(\frac{4}{3\pi}\frac{E}{Y}\tan\left(\frac{\pi}{2} - \theta\right)\right)\right], \text{for wedge geometry} \tag{7}$$

For example, the C_{ep} value of a 90° cutting-edge angle ($\theta = 45°$) wedge feature is 2.49, and the C_{ep} value of a 60° cutting-edge angle ($\theta = 30°$) wedge feature is 2.80 for the indentation of UHMWPE material. The assumption with constant E and Y is applied in this current model ($E = 1.4$ GPa, $Y = 25$ GPa).

To discuss the effect from viscoelasticity, we shall obtain the experimental penetration-depth data for UHMWPE. Wedge indenters (90° and 60° with 2 mm edge length) have been applied to the indentation tests in an earlier study.[7] The normal load was applied at strain rate of 0.1 s^{-1} and holds for 15 s. Given sufficient time (60 min) after the indentation tests, profiles of the indentation marks were measured by profilometry. The various normal loads were tested and the measured penetration depths were compared with the elastic-plastic calculation in Figure 4. We can also represent the experimental results by the following equation that is similar to that for the plastic and elastic-plastic calculations:

$$H_p = \frac{W}{2(C_{\mathrm{v}}Y)L_c \tan\theta} \tag{8}$$

where C_v is the coefficient for the viscoelastic UHMWPE from the experimental results. By comparing the elastic-plastic prediction results with the linear regression curve of the experimental results, we obtain

$$C_v = 1.75\ C_{\mathrm{ep}} \tag{9}$$

where C_{ep} is the coefficient for the elastic-plastic model. The penetration depth can be then predicted from the above equation after the viscoelastic properties are taken into account. It means the ratio of penetration depth predicted from the elastic-plastic assumption to the measured penetration depth is 1.75 ± 0.12 (mean ± standard deviation).

Figure 5 shows that the prediction from the calculation with elastic-plastic assumption is larger than the experimental measurements. It is suggested that the difference arises from the viscoelasticity of UHMWPE for the following possible reasons: (1) recovery of material deformation: after the indentation process, removal of the applied stress results in the gradually recovery of material deformation. (2) creep

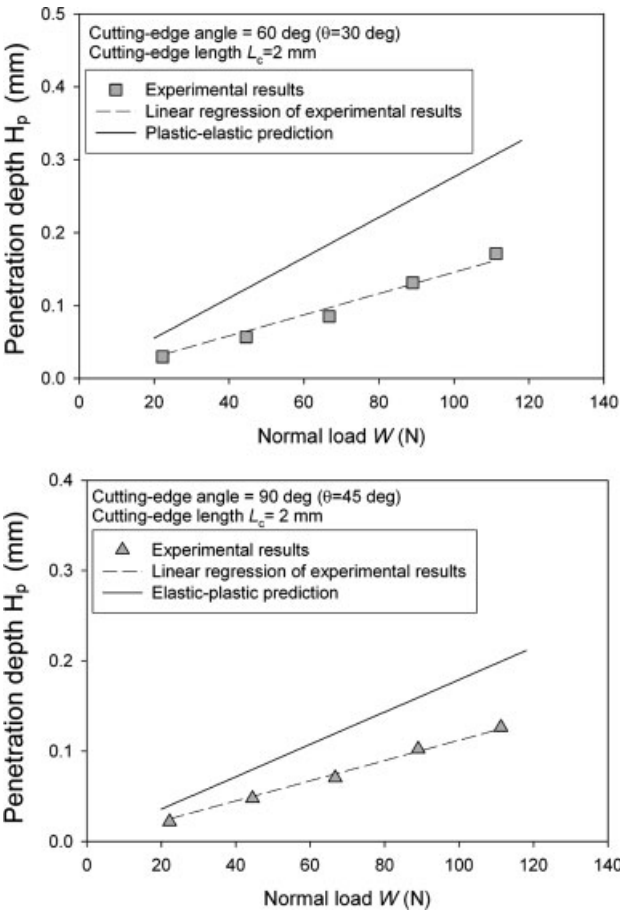

Figure 5 Comparison of the experimental data of wedge indentation in UHMWPE with elastic-plastic calculation results.

behavior during the indentation: for a viscoelastic material, the material deformation is a function of the strain rate. Under a high strain rate, the time allowed for material deformation is short and thus, the final material deformation is smaller than for the case with low strain rate under the same applied stress, and (3) strain hardening of the material: during the indentation process, the plastic deformation brings the strain hardening of the material. It leads to an increased material resistant during the indentation process and a smaller penetration depth.

The viscoelastic recovery of the material in the cutting-edge penetration process has a dramatic influence on the final penetration depth. We conclude that the final penetration depth can be estimated from eq. (8).

Lateral sliding process

During the sliding process, a horizontal displacement is applied to the cutting edge under a constant normal load and the material is lowered. A schematic representation of the process is shown in Figure 6. The introduction of the lateral sliding process unloads the left-hand face of the cutting edge. Further vertical deformation takes place by the cutting edge sliding further deeper in the sliding process. UHMWPE material displaced by the cutting edge was accumulated in front of the edge. The resultant force from the displaced volume acts on the cutting edge as an encountered force to the normal load. The net normal load is decreased and it leads to the decrease of the penetration depth. During the subsequent sliding process, the displaced volume for unit sliding distance is decreased. More volume is accumulated in front of the cutting edge with a decreasing rate of increase of displaced volume. It is an iterative process between increase of resistant force by increased displaced volume and decrease of penetration depth by the increase of material resistant force. Finally, the cutting edge is pushed away from the UHMWPE material and the displaced volume of UHMWPE is projected to be the volume of the generated particle. Calculation of the projected volume of the particle is based on various dimensions of cutting edges and mechanical loading conditions. Figure 7 shows a flow chart of the calculation procedure. With known L_c, W_c, H_c, and θ, the penetration depth can be calculated. During the sliding process, one face of the cutting edge was unloaded because of the horizontal sliding motion. The supporting area of the cutting edge is half of the area in an indentation process. Equation (8) is then modified as eq. (10) to calculate the penetration depth during the sliding process:

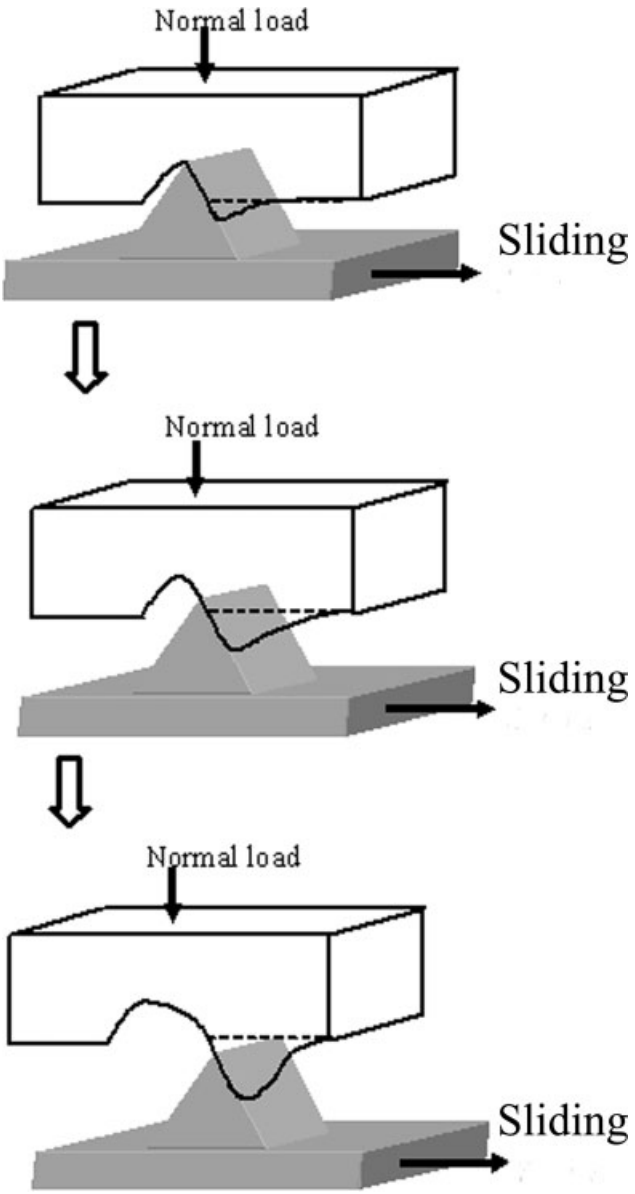

Figure 6 Schematic representation of the sliding process of the cutting edge.

$$H_{\mathrm{pc}} = \frac{W}{(C_v Y) L_c \tan \theta} \tag{10}$$

If the calculated penetration depth is larger than the feature height H_c, the real penetration depth is equal to the feature height. The minimum load W_m needed to reach the penetration depth H_c is then back calculated:

$$W_m = H_c (C_v Y) L_c \tan \theta \tag{11}$$

With a small increment of sliding distance, we can calculate the displaced volume by the product of cutting edge length, penetration depth and the incre-

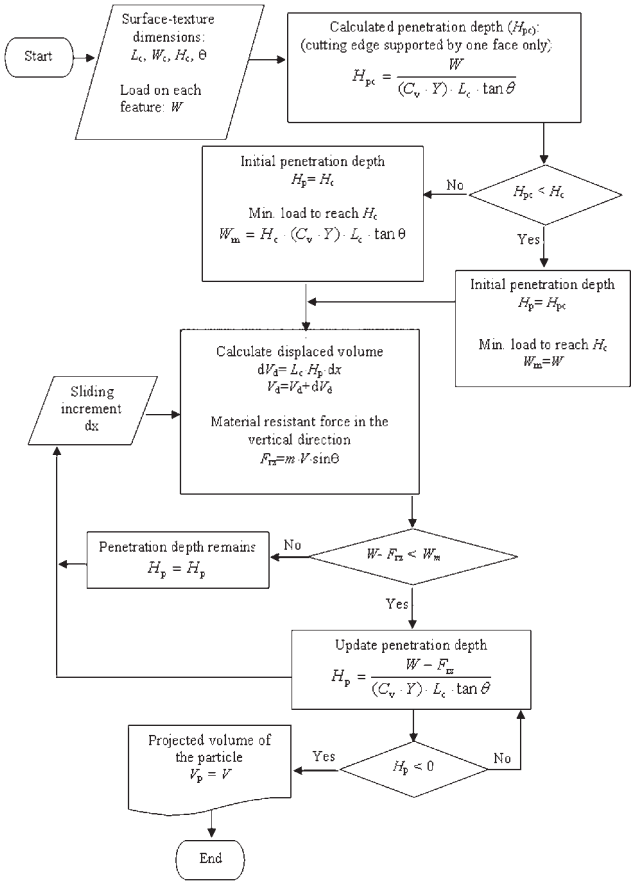

Figure 7 A flow chart of calculation of the sliding process of the cutting edge.

ment of sliding distance. With known quantity of displaced volume (V_d), the material resistant force can be estimated. From an earlier study,[6] the material resistant force per unit volume of UHMWPE was obtained as $m = 1.2\ 10^{-6}$ N/μm^3. The resolved resistant force in the vertical direction from the displaced volume of UHMWPE is calculated:

$$F_{rz} = F_r \sin\theta = mV_d \sin\theta \tag{12}$$

Obviously, the cutting-edge angle plays an important role at distributing the material resistant force in the vertical direction. With the same displaced volume, a larger force is distributed in the vertical direction for a larger cutting-edge angle. The penetration depth was then updated by the new normal load in the Eq. (13):

$$H_p = \frac{W - F_{rz}}{(C_v Y) L_c \tan\theta} \tag{13}$$

For the case with initial penetration depth equal to the feature height, there exists excess load between the cutting edge and UHMWPE material. The cutting edge needs to displace a larger volume of UHMWPE during the sliding process to generate sufficient resistant force to push away the cutting edge from the material surface.

After the penetration depth for a small increment of sliding distance is updated, the new penetration depth was then used to calculate the displaced volume in the next increment of sliding. Assuming incompressibility of the material, the accumulated displaced volume of UHMWPE was determined by adding up the displaced volume from each sliding increment. The iteration process was carried out until the penetration depth reaches zero. It indicates that the cutting edge was pushed away from the UHMWPE surface. The total displaced volume during the process is projected to the particle volume.

RESULTS

The model of particle generation was applied to predict the particle volume with given surface-texture dimensions and mechanical loading conditions. For the experimental results, the particle volume was estimated by the product of particle length, particle width, and particle thickness from the SEM observations in the earlier study.[6] The predictions by the model are compared with the experimental results. The effects of normal load, feature height, and cutting-edge angle are discussed.

Effect of normal load

Figure 8(a) shows the comparison of the model predictions and the experimental results from various normal loads based on the surface texture with dimensions of $L_c = 7.0$ μm, $W_c = 5.0$ μm, and $H_c = 3.0$ μm. Both results show that increase of load leads to a larger particle volume. The calculation results indicated that the minimum load (W_m) needed on each feature to reach the penetration depth equal to the feature height is only 0.0017 N. The loads applied in the earlier experiments were far larger than this value.[6] It means that the cutting edge was pushed to the end of the surface. Most of the material resistant force developed was used to encounter the excess load on the surface. Thus, a linear relationship between the normal load and particle volume is observed. However, the model predicted that particle volume is larger than the one from experimental results. In the model, we have assumed that the particle length is equal to the cutting-edge length. Previous experimental results demonstrate that the particle length is about 10–15% smaller than the cutting-edge length. The viscoelasticity, leading to the shrinkage of the particle dimension after the particle is released from the bulk UHMWPE, can explain some of the difference between predicted and the

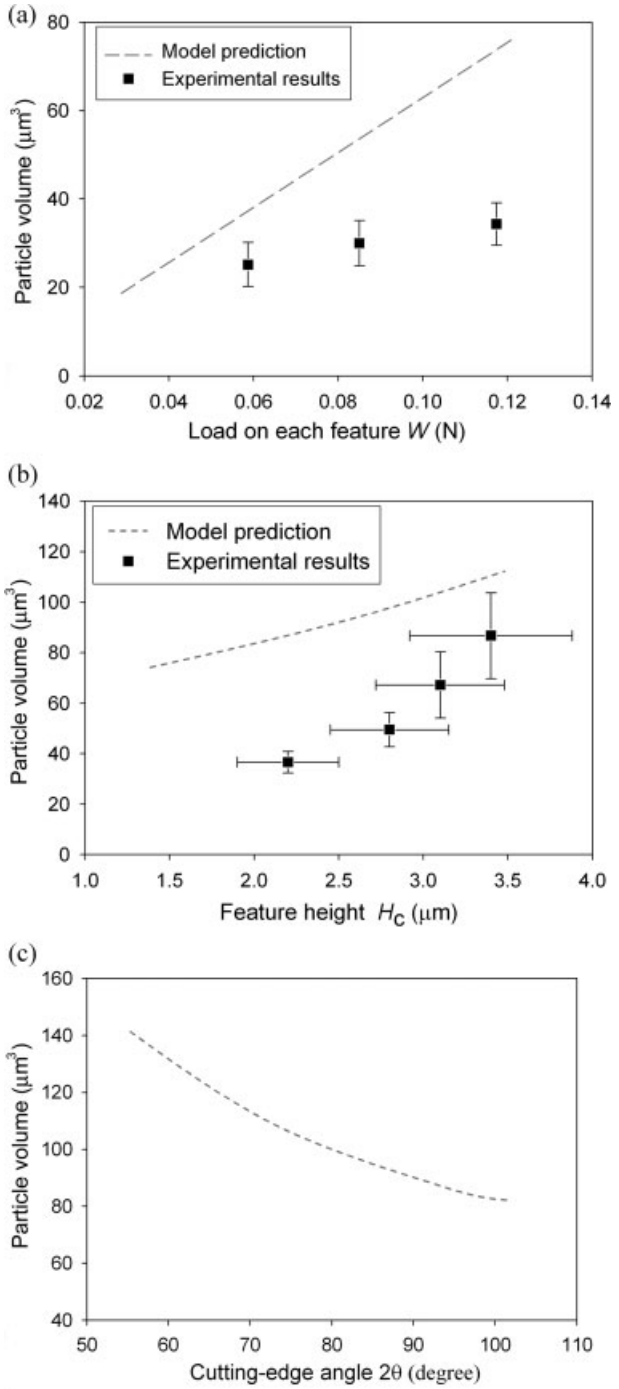

Figure 8 (a) Effect of normal load from model predictions and experimental results; (b) effect of feature height from model predictions and experimental results; (c) effect of cutting-edge angle from model calculations.

experimental results. On the other hand, the multiple surface features may reprocess the generated particles and further reduce the particle size. With the same feature density of the surface texture, there exists higher possibility for a larger particle to be reprocessed in the micro-cutting process. It is probably why we observed a larger difference between the model prediction and the experimental results for the larger particles.

Effect of feature height

Figure 8(b) illustrates the comparison of the model prediction and the experimental results from various feature height on the basis of the surface texture with dimensions of $L_c = 15.0$ μm, $W_c = 5.0$ μm, and two different feature heights with $H_c = 3.4$ and 2.8 μm. The mechanical condition of the tests include an average sliding speed of 57.2 m/s and a normal load of 96 N (load applied on each feature $W = 0.0587$ N). A larger feature height leads to a larger particle volume observed from the model predictions and experimental results. The applied load is also sufficient to push the cutting edge to the end of the surface. A larger feature height means a larger initial penetration depth at the beginning of the sliding process. Obviously, a larger penetration depth leads to a longer sliding distance and a larger particle volume. The results again show that the particle volume predicted by the model is larger than the experimental results. Figure 8(b) indicates that the difference between the model prediction and experimental results is smaller for a larger particle. Probably it is more difficult for the surface texture with a larger feature height to entrap the generated particles between the cutting edges and UHMWPE surface. Thus, less number of larger particles were reprocessed and so that the experimental results are closer to the model predictions, which are based on a single cutting-edge process.

DISCUSSION

There is a lack of experimental data with different cutting-edge angles, although maintaining the same feature height of the surface texture. The feature length $L_c = 15.0$ μm, feature height $H_c = 2.8$ μm, and normal load of 96 N (load applied on each feature $W = 0.0587$ N) were applied for the calculation process. By artificially changing the feature width in the model, the effect of cutting-edge angle on particle volume can be estimated. Figure 8(c) shows the particle volume versus different cutting-edge angles from the model calculations. A sharper cutting edge (smaller cutting-edge angle) results in a larger particle volume. With the same penetration depth, the sharper cutting edge leads to a longer sliding distance because a smaller material resistant force is distributed in the vertical direction to push away the cutting edge. Obviously, the predictions from the model are consistent with the theoretical approach of the particle-generation mechanism.

Slip-line field analyses have been applied to model the purely plastic deformation of metals of a wedge

sliding process.[10,11] Slip-line field analyses have provided the explanation of the movement of the wedge and the results are consistent with the experimental outcomes.[12] Under the purely plastic assumption of the slip-line field theory, the plastic deformation and strain takes place immediately when a stress which is larger than the yield criterion is induced. An elastic region of material response and the strain hardening behavior are neglected. However, for a relatively high-speed plastic deformation of a viscoelastic UHMWPE in the UHMWPE particle generation with surface textures, the strain hardening and the viscoelastic characteristics should be further taken into consideration in the model.

In this study, we have successfully established a mathematical model to describe the particle generation in an accelerated testing by rubbing UHMWPE with silicon surface with controlled asperities. The basic principle of force balance was adopted in the model. It should be noted that the viscoleastic effect of UHMWPE is not fully included in this model. Constant elastic modulus and yield strength assumptions were made in this study. By combining the indentation experimental data, the viscoelastic responses of UHMWPE under a specific strain rate is incorporated in the model. Therefore, the effect of sliding speed was not discussed in this calculation. This achievement enables us to predict the particle volume from a first principle approach. This model can assist on the design of surface textures to generate UHMWPE particles with desired size and shape. A correlation model obtained from the experimental results[6] shows that the experimental data can be predicted well by the following equation:

$$V_p = 39.5 \frac{L_c H_p^2 W^{0.6}}{S_p^{0.6}} (\text{unit} : \mu\text{m}, \text{N}, \text{s}) \qquad (14)$$

Both correlation and calculation models indicate the same trend of effects of surface-texture geometry and mechanical conditions on the volume of particles. However, the calculation model predicts a larger particle volume. To further quantitatively predict the particle volume precisely, the model should be further tightened to reflect the facts of multiple cutting edges and limited penetration depth in the real particle-generation process.

The original purpose of this series work is to generate UHMWPE wear particles for investigating the particles-induced immunological responses. In addition, we can adopt this idea to perform accelerated wear tests of materials. The uniformed surface asperities were fabricated on the material surface and applied in a linear reciprocating wear process to rub against the testing materials. By doing so, friction, wear rate, and wear particle morphology under a patterned stress situation can be observed and measured. The advantage is that the testing duration can be shortened into 1–2 days and the comparison of the wear rate can be made. By observing the wear particles retrieved from the tests, the lubrication mechanism can be easily investigated. An earlier study also adopted this procedure to investigate the biological lubrication on the wear of UHMWPE.[13] By further incorporating the model built up in this study, the role of various lubricants in wear prevention and friction reduction can be analyzed.

CONCLUSIONS

Microfabricated surfaces with controlled asperities have been applied to generate narrowly distributed UHMWPE wear particles with various sizes and shapes. A micro-cutting mechanism to generate particles was proposed. Contact mechanics model based on the calculation of the penetration depth and the displaced volume of UHMWPE iteratively from a force-balance basis was established in this study. A calculation procedure has been developed to predict the UHMWPE particle volume with a given surface-feature geometry and applied loads. The results of the model predictions are close to the experimental results of the particle generation.

The authors thank Dr. Stephen M. Hsu from National Institute of Standards and Technology and Professor Jan V. Sengers from University of Maryland for their comments and supports.

References

1. Harris, W. H. Clin Orthop Res 1995, 311, 46.
2. Amstutz, H. C.; Campbell, P.; Kossovsky, N.; Clarke, I. C. Clin Orthop Res 1992, 276, 7.
3. Maloney, W. J.; Smith, R. L. J Bone Joint Surg Am 1995, 77, 1448.
4. Fang, H.-W.; Hsu, S. M.; Sengers, J. V. Mat und Werk 2003, 34, 976.
5. Fang, H.-W.; Hsu, S. M.; Sengers, J. V. J Biomed Mater Res B: Appl Biomater 2003, 67, 741.
6. Fang, H.-W.; Hsu, S. M.; Sengers, J. V. NIST Special Publication 1002, 2003.
7. Fang, H.-W.; Hsu, S. M.; Sengers, J V. Polym Test 2006, 25, 424.
8. Yu, W.; Blanchard, J. P. J Mater Res 1996, 11, 2358.
9. Johnson, K. L. J Mech Phys Solids 1970, 18, 115.
10. Challen, J. M.; Oxley, P. L. B. Wear 1979, 53, 229.
11. Black, A. J.; Kopalinsky, E. M.; Oxley, P. L. B. J Phys D: Appl Phys 1993, 26, 1892.
12. Black, A. J.; Kopalinsky, E. M.; Oxley, P. L. B. Wear 1988, 123, 97.
13. Fang, H.-W.; Su, Y. C.; Huang, C. H.; Yang, C. B. Mater Chem Phys 2006, 95, 280.